Article

Active Manipulation of Quantum Dots using AC Electrokinetics

Mandy L. Y. Sin, Vincent Gau, Joseph C. Liao, David A. Haake, and Pak Kin Wong
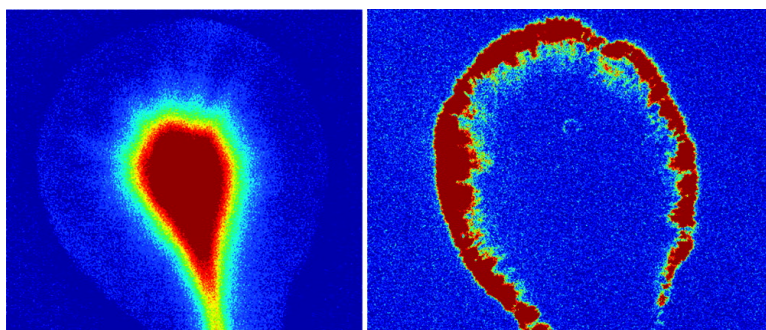
More About This Article

Additional resources and features associated with this article are available within the HTML version:

- Supporting Information
- Access to high resolution figures
- Links to articles and content related to this article
- Copyright permission to reproduce figures and/or text from this article

View the Full Text HTML

Active Manipulation of Quantum Dots using AC Electrokinetics

Mandy L. Y. Sin,[†] **Vincent Gau,**[‡] **Joseph C. Liao,**[§] **David A. Haake,**[||] **and Pak Kin Wong*,**[†,⊥]

Department of Aerospace and Mechanical Engineering, University of Arizona, Tucson, Arizona 85721; Genefluidics, Inc., Monterey Park, California 91754; Department of Urology and Bio-X Program, Stanford University, Stanford, California 94305; Department of Medicine, The David Geffen School of Medicine at UCLA and Division of Infectious Diseases, Veterans Affairs Greater Los Angeles Healthcare System, Los Angeles, California 90095; and Biomedical Engineering Interdisciplinary Program and Bio5 Institute, University of Arizona, Tucson, Arizona 85721

The superior optical and electrical properties of quantum dot (QD) nanoparticles are being applied in a new generation of QD devices for microelectronic, nanophotonic, and biomedical systems. Research on integrated QD-based systems has been focused on passive manipulation of QDs including template-guided self-assembly, molecular scaffold-based assembly, and microbead-based assembly. However, little effort has been devoted to development of methods for active manipulation, such as positioning and concentration, of QDs. In this study, we show that 20 nm colloidal QDs can be effectively positioned and concentrated using a combination of dielectrophoresis (DEP) and AC electro-osmosis (ACEO). The long-range fluid motion generated by ACEO entrains QDs to the area near the electrode surface, which facilitates the trapping of QDs by DEP. A systematic investigation was performed to examine electrokinetic processes at different applied frequencies and voltages using a concentric electrode configuration. We demonstrate that QDs can be dynamically positioned with an electric field strength as small as 10 kV/m and define the operating parameters for increasing the concentration of colloidal QDs by 2 orders of magnitude within one minute.

Introduction

Active manipulation of quantum dots (QDs) would greatly facilitate their integration in nanoscale optoelectronic and biomedical devices.[1−11] For example, concentration of colloidal QDs would provide an effective means to increase the signal level of QD biosensors.[12,13] An effective approach for manipulating nanoscale objects is alternating current (AC) electrokinetics, the application of an AC electric field to manipulate bulk fluids and embedded objects. AC electrokinetic techniques, such as dielectrophoresis (DEP)[14] and AC electro-osmosis (ACEO),[15−19] are ideal methods for manipulating nanoscale and biological objects such as colloidal particles, cells, viral particles, nucleic acids, and protein molecules.[15,20,21] Because of the small length scale, a relatively small applied voltage (typically a few volts) is required for AC electrokinetic manipulation. The combination of AC potential and low applied voltage avoids electrolysis and the problem of bubble formation observed in DC operation (e.g., electrophoresis). Despite these inherent advantages, little is known about the electrokinetic characteristics of colloidal QDs, and AC electrokinetic techniques have not been explored for active manipulation, such as concentration and positioning, of QDs.

AC electrokinetic techniques differ in their effects and effective force ranges. DEP is a particle force that acts directly on the embedded particle and is highly effective for short-range manipulation of particles.[15,20] In DEP, a dipole is induced in a polarizable particle when the particle is subjected to an electric field. If the electric field is nonuniform, the particle experiences a net force toward the high or low electric field region.[14] The time averaged dielectrophoretic force is given by

$$F_{DEP} = 2\pi R^3 \varepsilon \mathrm{Re}\{K(\omega)\}\nabla|E_{rms}|^2 \qquad (1)$$

where R is the particle radius, ε is the permittivity of the medium, E_{rms} is the root-mean-square electric field, ω is the angular field frequency, and $\mathrm{Re}[K(\omega)]$ represents the effective polarizability of the particle in the medium.[22]

ACEO is a second electrokinetic phenomenon that is effective in generating long-range fluid motion for micro- and nanoscale manipulation.[17] ACEO generates bulk fluid motion, which manipulates particles via hydrodynamic drag. The phenomenon was initially interpreted as negative DEP initially. Since the report of the phenomenon, several techniques were developed based on ACEO, such as an electrokinetic ratchet pump,[23] vortex micromixer,[24] and DNA concentrator.[25] When a potential is applied to the electrode, the field attracts charges to accumulate on the electrode surface, which changes the charge density near the electrode surface and forms an induced electric double layer (EDL). The amount of charges accumulated depends on the frequency of the applied potential. It should be noted that EDL can be formed without an applied potential. In the case of ACEO, the induced EDL interacts with the tangential component of the electric field to induce bulk fluid motion. In an alternating electric field, the sign of the charges in the EDL and the direction of the tangential component of the electric field both change. Therefore, the direction of the resultant force on the fluid

* To whom correspondence should be addressed. Phone: (520) 626-2215; Fax: (520) 621-8191; E-mail: pak@email.arizona.edu.
† Department of Aerospace and Mechanical Engineering, University of Arizona.
‡ Genefluidics, Inc.
§ Stanford University.
|| The David Geffen School of Medicine at UCLA and Division of Infectious Diseases.
⊥ Biomedical Engineering Interdisciplinary Program and Bio5 Institute, University of Arizona.
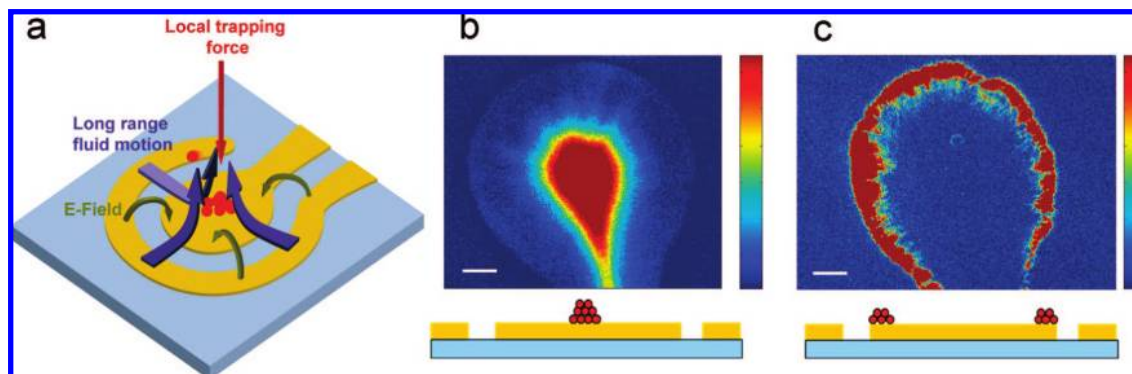
Figure 1. AC electrokinetic processor for active manipulation of colloidal QDs. (a) Schematics illustrating QD manipulation with a combination of electrohydrodynamic flow and local electrokinetic trapping force. (b) Trapping of QDs at the center of the inner electrode at higher frequency (6 V_{pp}, 300 Hz). Schematics of the side view of the concentration processes are inserted below the images. (c) Trapping of QDs at the edge of the inner electrode (6 V_{pp}, 40 Hz). Scale bars are 100 μm.

remains the same and generates a net fluid movement. By applying a linear double-layer approximation, it has been shown that the AC electroosmotic velocity v can be estimated to be

$$<v(r)> \; = \frac{1}{8}\frac{\varepsilon V_0^2\Omega^2}{\mu r(1 + \Omega^2)^2} \tag{2}$$

where V_0 is the amplitude of the AC potential, μ is the viscosity of the electrolyte, and r is the distance from the center of the electrode gap for a parallel electrode.[16] The nondimensional frequency Ω is given by

$$\Omega = \omega r\frac{\varepsilon}{\sigma}\frac{\pi}{2}\kappa \tag{3}$$

where σ is the conductivity of the medium and κ is the reciprocal Debye length of the EDL. The velocity formula predicts that the AC electroosmotic flow increases with the second power of the applied voltage and has a maximum at an intermediate frequency.[16,17,25,26] A detailed description of ACEO (Sections 1–3 of the Supporting Information) and a video for visualization of the fluid motion generated by ACEO are included in the Supporting Information.

Experimental Methods

Materials. QD samples in the experiments were carboxyl modified QDs (Qdot 525 ITK, Invitrogen). The QDs were diluted to 5 nM with DI water and adjusted to a conductivity of 0.7 mS/m. Microscopic inspection was performed before all the experiments, and we did not observe QD aggregation at this condition. The electrode configuration for QD manipulation is shown in Figure 1a. The electrode design comprises a concentric outer electrode and a circular inner electrode. The diameter of the outer electrode is 1.5 mm, and the gap distance is 200 μm. The gold electrodes were fabricated by sputtering on polyethylene terephthalate (PET) substrates with a shadow mask. To create a microfluidic chamber, two spacers of 170 μm in length were first placed on top of both sides of the electrode. A droplet of 2 μL of QD solution was then pipetted onto the electrode surface and covered with a coverslip (Fisher Sci). AC electrical signal was provided by a function generator (HP, 33120A). The outer electrode was connected to the ground, and the inner electrode was connected to the driving signal.

All the voltage values reported are peak-to-peak amplitude of the driving signal.

Imaging. The electrokinetic chip was loaded onto a digital inverted epifluorescence microscope (DMI 4000B, Leica Microsystems). Samples were illuminated at a wavelength of 515–560 nm with a mercury vapor lamp, and images were recorded above 590 nm. All experiments were performed at room temperature. The dynamics of QDs concentration were recorded by a CCD camera and directly digitized into a video capture system.

Data Analysis. The images and videos were processed by NIH ImageJ software. Fluorescent intensity was normalized by the initial intensity before the application of the AC potential. Data of QD kinetics were smoothed out by weighted averages with its nearest neighbor of $x_i = 0.33x_{i-1} + 0.34x_i + 0.33x_{i+1}$. Data are reported as mean ± standard deviation for at least three consecutive experiments. Peak frequencies of the positioning processes were determined by fitting the data with a Gaussian profile (Origin, OriginLab Inc.). The scaling dependences of applied voltage were determined by regression analysis and presented as mean ± standard error in the slope of the fit.

Results and Discussion

AC electro-osmotic flow is a surface driven effect; therefore, proper electrode design (e.g., electrode surface area, electrode gap distance, and geometry) is essential to formation of desired flow patterns in electrokinetic manipulation studies. The electrode surface area has to be large enough to generate long-range fluid motion while it also has to be small enough to produce a strong enough electric field. To actively manipulate colloidal QDs, we designed a concentric electrode configuration[25–29] (Figure 1a). In this design, the large surface area of the inner electrode generates long-range fluid movement by ACEO (see Section 4 of the Supporting Information for a comparison between the concentric electrode configuration and a parallel electrode design). The flow transports the embedded QDs in the bulk fluid to the area near the electrode surface. The bulk fluid flow permits a large effective region for QD manipulation while DEP allows trapping of the QDs on the electrode surface. We have also tested larger electrodes, which show weaker trapping effects as a result of small electric field strengths. By optimizing the applied voltage and frequency, we observed that the QDs can be positioned at two equilibrium locations, which are the edge and the center of the inner electrode. Figure 1b and c shows typical electrokinetic manipulation experiments at

Active Manipulation of Quantum Dots

J. Phys. Chem. C, Vol. 113, No. 16, 2009 **6563**
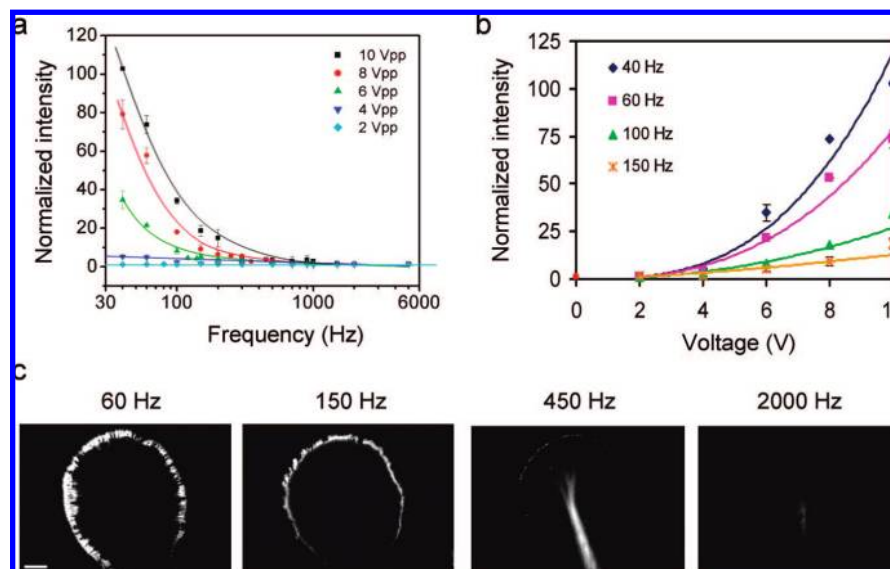
Figure 2. Electrokinetic concentration of QDs at the edge of the inner electrode. (a) Frequency dependence of the concentration process at different voltages. (b) Voltage dependence of the concentration process at different frequencies. The scaling exponents were determined to be 2.93 ± 0.26 (at 40 Hz), 2.63 ± 0.20 (at 60 Hz), 2.12 ± 0.29 (at 100 Hz), and 1.47 ± 0.38 (at 150 Hz). (c) Concentration of QDs at different frequencies. Scale bar is 100 μm.

steady state (see also Videos S1 and S2 of the Supporting Information).

The fluorescence intensities (i.e., concentration of the QDs) were measured at the edge and the center of the inner electrode in order to investigate the voltage and frequency dependencies. The frequency dependence of the concentration process at the edge is shown in Figure 2a. The QDs were concentrated at the edge at low frequency (<500 Hz), and their concentration increased by over 100-fold at 10 V_{pp} (peak to peak) and 40 Hz. Because the electrode edge has the strongest electric field gradient, the accumulation of the QDs at this location indicates that DEP plays a dominant role in the concentration process. Similar frequency dependent effects have also been reported for DEP trapping of small DNA molecules.[30,31] We further examined the voltage dependence of the concentration process. Fluorescence intensity increased with the applied voltage with a range of scaling exponents depending on the frequency (Figure 2b). The exponents are significantly different from the square dependence expected for DEP (see eq 1), and the values decrease with the increase in applied frequency (2.93 ± 0.26 at 40 Hz, 2.63 ± 0.20 at 60 Hz, 2.12 ± 0.29 at 100 Hz, and 1.47 ± 0.38 at 150 Hz). It should also be noted that the edge of the outer electrode, which has smaller surface area, shows little to no QD accumulation. A likely explanation is that other electrokinetic phenomena (e.g., electric field-induced particle−particle interactions, particle−surface interactions, and electrohydrodynamic flows) contribute to the concentration process.

The kinetics of the concentration process was measured to investigate the contribution of other electrokinetic phenomena. Figure 3a shows the normalized intensity near the electrode edge at different frequencies. The increase in intensity upon application of the AC electric field can be fitted by a single-exponential function $(1 - e^{-t/\tau})$. The time constant τ shows a strong dependence on the applied frequency (Figure 3b) and is minimized at an intermediate frequency, which correlates well with the frequency dependence of ACEO.[17,25,26] Figure 3c shows a video time series of the concentration process near the electrode edge. We observed strong fluid motion on the electrode surface during the concentration process and the QDs could be pushed toward the center of the inner electrode (see Videos S1

and S2 of the Supporting Information). The frequency dependence of the concentration rate indicates that ACEO is one of the primary contributors to the concentration process.

We also measured the fluorescent intensity at the center of the inner electrode. The QDs were drawn toward the center of the electrode at higher frequencies. At a given applied voltage (e.g., 10 V_{pp}), the concentration process was insignificant at high and low frequencies (larger than 2000 Hz or smaller than 100 Hz) and was maximized at intermediate peak frequencies (400 Hz) (Figure 4a). The frequency-dependent effect was strongly correlated with the AC electro-osmotic velocity. The local concentration at the center increased approximately by a factor of 5. Peak fluorescence intensity showed only a weak dependence on the applied voltage. The manipulation of the QDs was achievable with as small as 2 V_{pp} (electric field of 10 kV m^{-1}). Optimal frequency was found to increase with the applied voltage (Figure 4b). Figure 4c shows a video time series of the positioning process. These observations can be qualitatively understood by the force balance between DEP and ACEO. Trapping of QDs requires that the hydrodynamic drag force is balanced by the DEP trapping force. An increase in voltage increases both the strength of DEP and ACEO; therefore, the concentration process shows only a weak dependence on the applied voltage. Nevertheless, the electric field dependencies for DEP and for the hydrodynamic drag generated by ACEO could be different for QDs (see Figure 2b). Therefore, the optimal frequency for trapping QDs shifts in order to maintain the force balance at different voltages.

DEP is known to be effective for manipulating micrometer scale objects; however, the force generated is often insufficient for manipulating smaller objects ($F_{DEP} \sim R^3$). The effectiveness of the approach described here for concentration of 20 nm QDs by 2 orders of magnitude is likely to be a result of combined DEP and ACEO effects. The approach is substantially more effective than conventional DEP concentrators, which only increase the concentration by a factor of less than 5 for small DNA molecules.[31] We have tested a parallel electrode configuration to concentrate QDs with DEP (Figure S4 of the Supporting Information). Our concentric electrode configuration shows a 30-fold improvement compared to the parallel plate
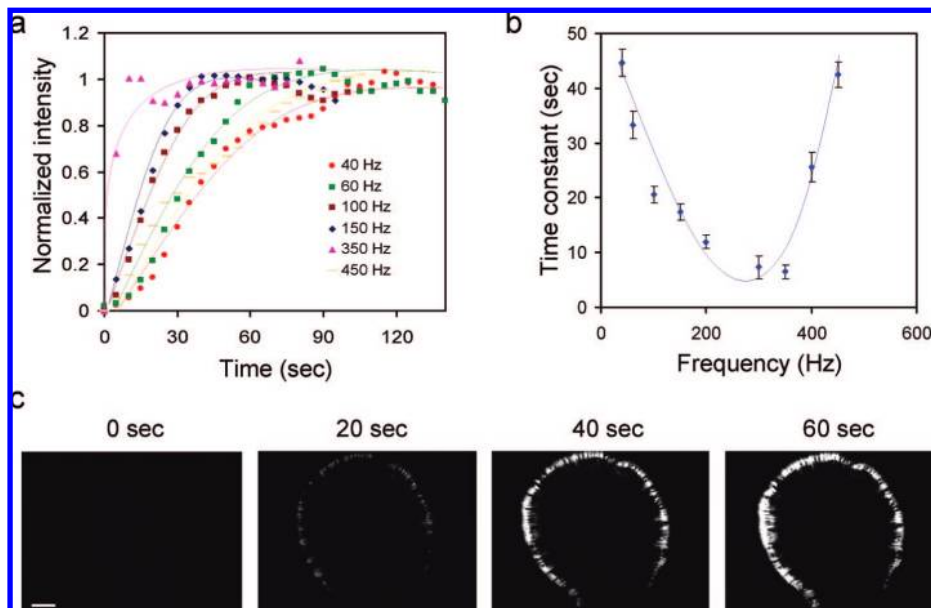
Figure 3. Kinetics of the QD concentration process at the edge. (a) Kinetics of the concentration process at different frequencies. The applied voltage was 10 V_{pp}. (b) Frequency dependence of the concentration process at 10 V_{pp}. The smallest time constant for the concentration process is approximately at 300 Hz. (c) Video time series of the concentration process (8 V_{pp}, 400 Hz). Scale bar is 100 μm.
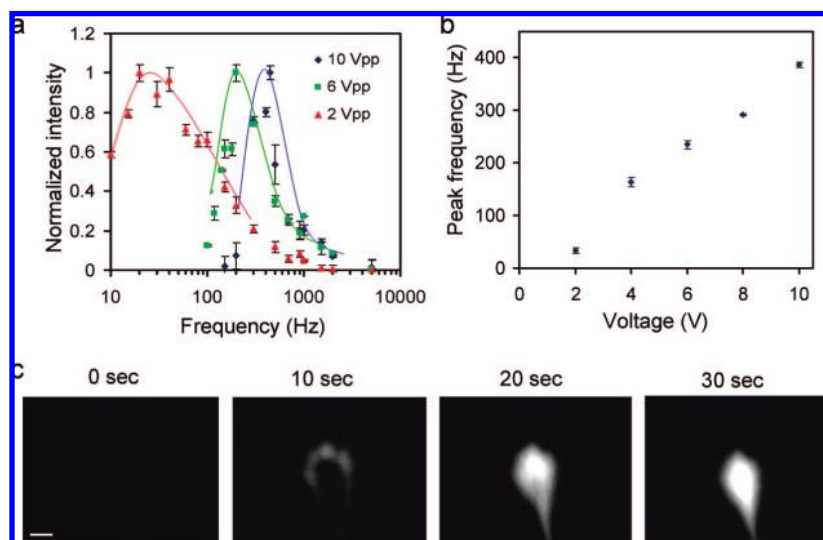
Figure 4. Electrokinetic positioning of QDs at the center of the inner electrode. (a) Frequency dependence of the concentration process at different voltages. The concentration effect showed only a weak dependence on the applied voltage, and the data were normalized by the peak intensity to compare the frequency dependence. (b) Voltage dependence of the peak frequency for positioning the QDs at the center of the inner electrode. (c) Video time series of the positioning process on the inner electrode surface (2 V_{pp}, 40 Hz). Scale bar is 100 μm.

electrode. This further indicates the important role of ACEO, which is a surface-driven phenomenon, in the active manipulation process. Recently, dynamic manipulation of nanowires 20 nm in diameter and 5 μm in length has been demonstrated using optoelectronic tweezers, which is based on photopatterned virtual electrodes and DEP.[6,21] The QDs used in our study are 250 times smaller in dimension than the nanowires used in that report.

The superior properties of metallic nanoparticles and nanotubes have been applied in various advanced nanoengineered systems for microelectronic, nanophotonic, and biomedical applications.[32−36] Effective manipulation techniques for these entities will contribute significantly for fully utilizing their potentials and development of functional engineering systems. Electrokinetic manipulation of metallic nanoparticles and nanotubes has been reported using small electrodes or other approaches that generate significantly larger electric field gradient in small areas.[37−39] These devices typically require electric field

strengths on the order of 0.1−1 MV m^{-1}. In this study, our technique manipulates QDs in a large region with an electric field strength of 10 kV m^{-1}, which is 1−2 orders of magnitude smaller than typical DEP manipulators. The effectiveness of our device is a result of the combination of the long-range ACEO and the short-range DEP. Our device can potentially be applied for the manipulation of other nanoscale entities.

Conclusion

In conclusion, the findings reported here would have broad impacts on AC electrokinetic-assisted assembly of QDs and other nanoparticles for integrated nanosystems. For example, the ability to increase the concentration of nanoscale objects by over 2 orders of magnitude could be applied to amplify the signal level of nanoparticle and QD-based biosensors. We have previously shown that electrochemical biosensors with concen-

Active Manipulation of Quantum Dots

J. Phys. Chem. C, Vol. 113, No. 16, 2009 **6565**

tric electrode configurations may be used for rapid molecular identification of pathogens.[28,40] The electrokinetic bioprocessor described herein may be integrated with the electrochemical biosensor to facilitate concentration and mixing of target analytes with surface-immobilized recognition elements such as DNA oligonucleotide probes, antibodies, or aptamers. The current investigation of QD manipulation will form the foundation for rationalizing the manipulation of QD bioconjugates and optimizing the operating parameters. Efficient molecular manipulation has the potential to dramatically shorten the detection time and improve sensitivity.

Supporting Information Available: Videos of active manipulation of QDs at the edge and at the center of the inner electrode. A video for visualizing the ACEO flow. Description of ACEO and comparison of different electrode geometries. This information is available free of charge via the Internet at http://pubs.acs.org.

References and Notes

(1) Wang, C. J.; Huang, L.; Parviz, B. A.; Lin, L. Y. *Nano Lett.* **2006**, *6*, 2549.
(2) Zhang, C. Y.; Yeh, H. C.; Kuroki, M. T.; Wang, T. H. *Nat. Mater.* **2005**, *4*, 826.
(3) Alivisatos, A. P. *Science* **1996**, *271*, 933.
(4) Freeman, R.; Gill, R.; Beissenhirtz, M.; Willner, I. *Photochem. Photobiol. Sci.* **2007**, *6*, 416.
(5) Kongkanand, A.; Tvrdy, K.; Takechi, K.; Kuno, M.; Kamat, P. V. *J. Am. Chem. Soc.* **2008**, ASAP article.
(6) Jamshidi, A.; Pauzauskie, P. J.; Schuck, P. J.; Ohta, A. T.; Chiou, P. Y.; Chou, J.; Yang, P. D.; Wu, M. C. *Nat. Photonics* **2008**, *2*, 85.
(7) Hegg, M.; Lin, L. Y. *Opt. Express* **2007**, *15*, 17163.
(8) Badolato, A.; Hennessy, K.; Atature, M.; Dreiser, J.; Hu, E.; Petroff, P. M.; Imamoglu, A. *Science* **2005**, *308*, 1158.
(9) Tang, Z. Y.; Wang, Y.; Kotov, N. A. *Langmuir* **2002**, *18*, 7035.
(10) Lee, S. W.; Mao, C. B.; Flynn, C. E.; Belcher, A. M. *Science* **2002**, *296*, 892.
(11) Han, M. Y.; Gao, X. H.; Su, J. Z.; Nie, S. *Nat. Biotechnol.* **2001**, *19*, 631.
(12) Yeh, H. C.; Ho, Y. P.; Shih, I. M.; Wang, T. H. *Nucleic Acids Res.* **2006**, *34*.
(13) Maxwell, D. J.; Taylor, J. R.; Nie, S. M. *J. Am. Chem. Soc.* **2002**, *124*, 9606.
(14) Pohl, H. A. *J. Appl. Phys.* **1951**, *22*, 869.
(15) Ramos, A.; Morgan, H.; Green, N. G.; Castellanos, A. *J. Phys. D: Appl. Phys.* **1998**, *31*, 2338.
(16) Ramos, A.; Morgan, H.; Green, N. G.; Castellanos, A. *J. Colloid Interface Sci.* **1999**, *217*, 420.
(17) Green, N. G.; Ramos, A.; Gonzalez, A.; Morgan, H.; Castellanos, A. *Phys. Rev. E* **2000**, *61*, 4011.
(18) Gonzalez, A.; Ramos, A.; Green, N. G.; Castellanos, A.; Morgan, H. *Phys. Rev. E* **2000**, *61*, 4019.
(19) Green, N. G.; Ramos, A.; Gonzalez, A.; Morgan, H.; Castellanos, A. *Phys. Rev. E* **2002**, *66*.
(20) Wong, P. K.; Wang, T. H.; Deval, J. H.; Ho, C. M. *IEEE/ASME Trans. Mechatronics* **2004**, *9*, 366.
(21) Chiou, P. Y.; Ohta, A. T.; Wu, M. C. *Nature* **2005**, *436*, 370.
(22) Jones, T. B. *Electromechanics of Particles*; Cambridge University Press: New York, 1995.
(23) Brown, A. B. D.; Smith, C. G.; Rennie, A. R. *Phys. Rev. E* **2001**, 6302.
(24) Huang, S. H.; Wang, S. K.; Khoo, H. S.; Tseng, F. G. *Sens. Actuators, B* **2007**, *125*, 326.
(25) Wong, P. K.; Chen, C. Y.; Wang, T. H.; Ho, C. M. *Anal. Chem.* **2004**, *76*, 6908.
(26) Bown, M. R.; Meinhart, C. D. *Microfluidics Nanofluidics* **2006**, *2*, 513.
(27) Fatoyinbo, H. O.; Hoettges, K. F.; Reddy, S. M.; Hughes, M. P. *Biosens. Bioelectron.* **2007**, *23*, 225.
(28) Liao, J. C.; Mastali, M.; Gau, V.; Suchard, M. A.; Moller, A. K.; Bruckner, D. A.; Babbitt, J. T.; Li, Y.; Gornbein, J.; Landaw, E. M.; McCabe, E. R. B.; Churchill, B. M.; Haake, D. A. *J. Clin. Microbiol.* **2006**, *44*, 561.
(29) Liao, J.; Mastali, M.; Li, Y.; Gau, V.; Suchard, M. A.; Babbitt, J.; Gornbein, J.; Landaw, E. M.; McCabe, E. R. B.; Churchill, B. M.; Haake, D. A. *J. Mol. Diagnost.* **2007**, *9*, 158.
(30) Chou, C. F.; Tegenfeldt, J. O.; Bakajin, O.; Chan, S. S.; Cox, E. C.; Darnton, N.; Duke, T.; Austin, R. H. *Biophys. J.* **2002**, *83*, 2170.
(31) Asbury, C. L.; van den Engh, G. *Biophys. J.* **1998**, *74*, 1024.
(32) Rosi, N. L.; Mirkin, C. A. *Chem. Rev.* **2005**, *105*, 1547.
(33) Zheng, Y. B.; Juluri, B. K.; Mao, X. L.; Walker, T. R.; Huang, T. J. *J. Appl. Phys.* **2008**, *103*.
(34) Hsiao, V. K. S.; Zheng, Y. B.; Juluri, B. K.; Huang, T. J. *Adv. Mater.* **2008**, *20*, 3528.
(35) Yu, C. X.; Irudayaraj, J. *Anal. Chem.* **2007**, *79*, 572.
(36) Huang, H. J.; Pierstorff, E.; Osawa, E.; Ho, D. *ACS Nano* **2008**, *2*, 203.
(37) Zheng, L. F.; Li, S. D.; Brody, J. P.; Burke, P. J. *Langmuir* **2004**, *20*, 8612.
(38) Hermanson, K. D.; Lumsdon, S. O.; Williams, J. P.; Kaler, E. W.; Velev, O. D. *Science* **2001**, *294*, 1082.
(39) Chan, R. H. M.; Fung, C. K. M.; Li, W. J. *Nanotechnology* **2004**, *15*, S672.
(40) Liao, J. C.; Mastali, M.; Li, Y.; Gau, V.; Suchard, M. A.; Babbitt, J.; Gornbein, J.; Landaw, E. M.; McCabe, E. R. B.; Churchill, B. M.; Haake, D. A. *J. Mol. Diagnost.* **2007**, *9*, 158.